Study of Pressure Distribution Along Supersonic Magnetohydrodynamic Generator Channel

G. D. Roy* and Y. C. L. Wu†
University of Tennessee Space Institute, Tullahoma, Tenn.

Static pressure and Hall voltage measurements were made in supersonic magnetohydrodynamic generators. Three identically sized generator channels, two of diagonal conducting wall design with sidewall angles of 45° and 60°, and one Hall type were used. The pressure rise (relative to the non-MHD case) increases with increasing load. The pressure rise of all three generators were similar although the Hall channel generated only about 1/3 of the power of the other two. The measured pressure distribution showed the existence of shocks in the generator at higher interactions. (The interaction parameter is approximately equal to 0.36). As the load increases the shock waves move toward upstream.

I. Introduction

THE principle of MHD power generation is the same as the conventional rotating machines (i.e., an electromotive force is induced resulting from conductors cutting magnetic field lines). In MHD power generators, the conductor is a plasma rather than metal wires as used in the rotating machines. The velocity and electrical conductivity of the plasma are, thus, most crucial in MHD power generation. Therefore, it is necessary to have as accurate a knowlege as possible of the working fluid. However, there are only very limited experimental data on the fluid mechanical behavior of MHD generators.[1-3]

This paper presents wall-pressure and Hall-voltage measurements along three conducting wall generators with sidewall angles of 90° (Hall), 60°, and 45° (DCW), respectively. A quasi-one-dimensional analysis with chemical reactions, friction effects and heat transfer is also made. Interpretation of the experimental results is given.

II. Experimental Setup and Conditions

The combustion-gas MHD generator experimental setup includes a fuel system where fuel, oxidizer, and seed are fed into a rocket-type combustor. The resulting combustion gas is expanded through a converging-diverging nozzle to a designated Mach number. The plasma then enters the generator channel and finally exhausts through a diffuser. Figure 1 shows the experimental setup schematically.

Two diagonal conducting wall generators, with sidewall angles of 45°, 60°, and one Hall (90°) generator were used in the experimental investigation. They have identical inside dimensions with a height of 4 in. at entrance diverging uniformly to 6 in. at exit (which corresponds to a wall divergence of 1.2°) and a constant width of 2 in. The parallel walls are in the direction of the applied magnetic field. The total length of the channel is 48 in., with an active generator section of 36 in. containing an assembly of 60 frame electrode elements insulated from each other. The remaining 12 in. of the channel length, (6 in. on each end) was made of blocks, electrically insulated from each other to serve as transition sections. For the Hall generator the electrode elements are 0.582 in. thick copper slabs electrically insulated from each other by 0.018 in. thick mica paper and arranged perpendicular to the axis of the channel. In the 45° and 60° slant-wall channels, the segments are made of 0.417 in. and 0.520 in. thick copper slabs, respectively. They are inclined at angles of 45° and 60°, respectively, to the channel axis. Therefore, the axial length (0.582) of all electrode elements for the three different generators is identical.

The working fluid is the product of RP-1 burned in oxygen and seeded with potassium hydroxide (KOH) dissolved in ethyl alcohol. The oxygen fuel ratio is stoichiometric and the seed concentration is one percent by weight of potassium. The total mass flow rate is 0.795 kg/sec. Combustion gas expanded from the combustor through a Mach 1.6 nozzle and then entered the MHD generator channel. The entrance temperature and pressure were 2750° K and 14 psia, respectively and the average combustor pressure was 46 psia. A conventional iron-core magnet capable of producing a maximum field strength of 2 Tesla (wb/m^2) was used.

The channels are of heat sink design. The channel wall temperature was approximately 500° K. The run time for each test was approximately 15 sec and the generated power was dissipated through a resistor load bank.

A total of 36 static pressure measurements were made at more than 12 different axial locations of the channel, with pressure taps located in the top, bottom, and sidewalls of the channel.

In addition to the static pressure measurements, the oxygen, fuel, and seed solution flow rates, as well as the combustor chamber pressure were measured. Load current, electrode current, total Hall voltage, and the incremental Hall voltage generated between adjacent electrodes were also measured. The Hall and 60° generators were loaded with a single load (two terminal connected), while the 45° generator was connected with multiple loads.

The nominal experimental conditions are: a) generator entrance Mach number = 1.6; and b) combustor pressure = 46.5 psia. The various flow rates are: $\dot{m}_{O_2} = 1.283$ lb/sec; $\dot{m}_{RP-1} = 0.365$ lb/sec; and $\dot{m}_{seed} = 0.116$ lb/sec, which yields approximately 1% of postassium by weight.

Under these conditions, the average flow parameters of the plasma in the generator channel are: velocity $u = 1200$ m/sec; density $\rho = 0.1$ kg/m^3; conductivity $\sigma = 12$ mhos/m; Hall parameter $\Omega = 1$; magnetic field $B = 2$ Tesla; active channel length $L = 36$ in. This gives an interaction parameter of 0.36 and magnetic Reynolds number of 0.016.

Presented as Paper 74-508 at the AIAA 7th Fluid and Plasma Dynamics conference, Palo Alto, Calif., June 17-19, 1974; submitted September 25, 1974; revision received March 10, 1975. This research is sponsored by the Office of Coal Research of the U.S. Department of the Interior and the Tennessee Valley Authority, Contract 14-32-0001-1213 and the Office of Scientific Research, USAF, Contract F44620-69-C 0031.

Index category: Plasma Dynamics and MHD.

*Graduate Research Assistant. Student Member AIAA.

†Professor of Aerospace Engineering. Associate Fellow AIAA.

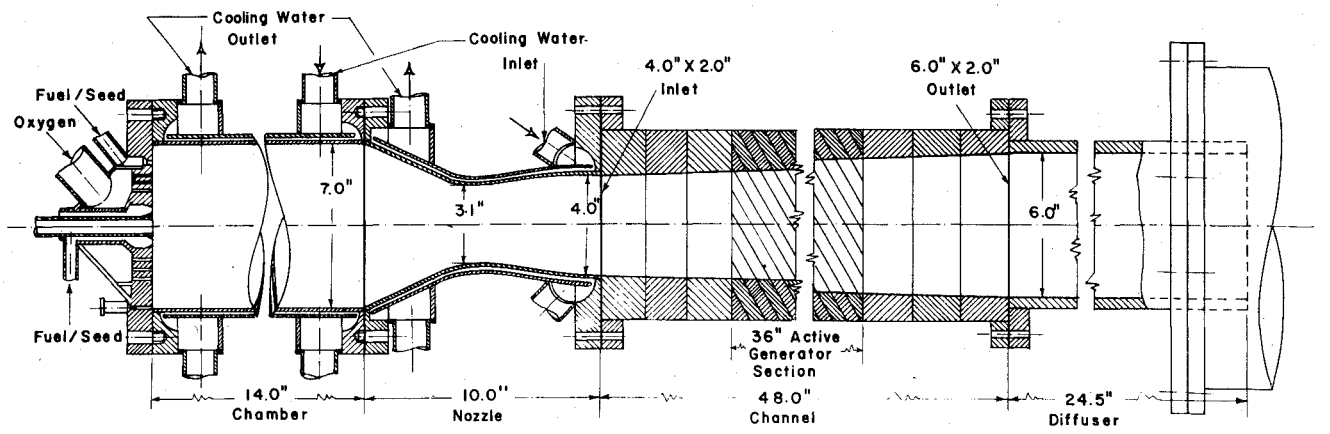

Fig. 1 Schematic of MHD generator assembly.

III. Analysis

A quasi-one-dimensional analysis including chemical reaction, friction and heat transfer was made.[4-5] Using the conventional nomenclature, the following equations describe the generator performance:

$$\rho uA = \dot{m} \tag{1}$$

$$\rho u(\mathrm{d}u/\mathrm{d}x) + (\mathrm{d}p/\mathrm{d}x) = -j_y B - \mathrm{d}X \tag{2}$$

$$\rho u\ (\mathrm{d}/\mathrm{d}x)\ (h + u^2/2) = \boldsymbol{j}\cdot\boldsymbol{E} + \mathrm{d}Q \tag{3}$$

and

$$p = p\ (h,s) \tag{4}$$

where ρ is the mixture density and h is the mixture enthalpy, which are calculated based on chemical equilibrium. The friction force $\mathrm{d}X$ and heat transfer $\mathrm{d}Q$ are adopted from empirical correlations for rough surfaces.[6] The electric field intensity $\boldsymbol{E}$ and current density $\boldsymbol{j}$ for a two-terminal connected generator can be written as,[7]

$$j_x = [-A\ \sigma uB\ (1-\Delta)\varphi + (1+\Omega\varphi)I]/[A(1+\varphi^2)] \tag{5}$$

$$j_y = [A\sigma uB(1-\Delta) - (\Omega-\varphi)\ I]/[A\ (1+\varphi^2)] \tag{6}$$

$$E_x = [-A\sigma uB(1-\Delta)\ (\Omega+\varphi) + (1+\Omega^2)\ I]/[A(1+\varphi^2)\sigma] \tag{7}$$

$$E_y = (\tan\theta)\ E_x = \varphi E_x \tag{8}$$

Here σ and Ω are electrical conductivity and Hall parameter respectively, θ is the angle of the normal of the conducting sidewall, and Δ is the dimensionless voltage drop defined as $\Delta = V_\mathrm{d}/uB\mathrm{d}$, where V_d is the voltage drop. The load current I is defined by

$$I = \boldsymbol{j}\cdot\boldsymbol{A} = (j_x + \varphi j_y)A \tag{9}$$

which is constant over each slant cross section for two terminal connection.

The quasi-one-dimensional equations together with the chemical, electrical, and thermodynamic relationships, can be integrated numerically for any given generator configuration with appropriate initial conditions, provided that the electrode voltage drop V_d is known. Constant V_d is assumed along the generator channel and its value is determined empirically by matching the total power output of the generator to measured values. From the measured pressure and mass flow, the Mach number was calculated at various axial locations along the channel. In cases of higher MHD interactions, it was found that the flow became subsonic toward the end of the channel, indicating presence of shocks. To investigate flows with the presence of shocks qualitatively, the computation was modified as follows. From the measured pressure distribution, a normal shock was inserted at the location of the peak pressure. The generator performance equations were solved up to the shock location. As the conditions just ahead of the shock are known, those after the shock were calculated by simultaneously solving the continuity, momentum, and energy equations. Then with conditions after the shock as initial conditions, the generator equations were integrated until the end of the channel.

IV. Results and Discussion

A. Non-MHD Pressure Distribution

Figure 2 shows the pressure distribution along a Hall generator when the magnetic field was absent. For the same axial location, deviations are noted in the pressures recorded at the top, side, and bottom probes. The differences in pressures are directly resulted from the segmentation roughness which is of the order of 0.5 mm. In the Hall configuration, the top, side, and bottom probes are located in the same electrode element. Therefore, if the bottom of the electrode element is recessed from its neighboring upstream wall, then this electrode bottom wall will form a long shallow cavity. On the top side of the channel, the electrode wall then forms a small forward step. Figure 3 shows schematically the wave systems existing in such a configuration. The ratio of the electrode length and the average segmentation step height is approximately 30. The pressure tap is located in the middle of the electrode element. The different pressures sensed by the top and bottom pressure taps indicate that the pressure has not yet recovered back to its "freestream" value. Therefore, the cavity side (bottom pressure as shown in Fig. 3) will

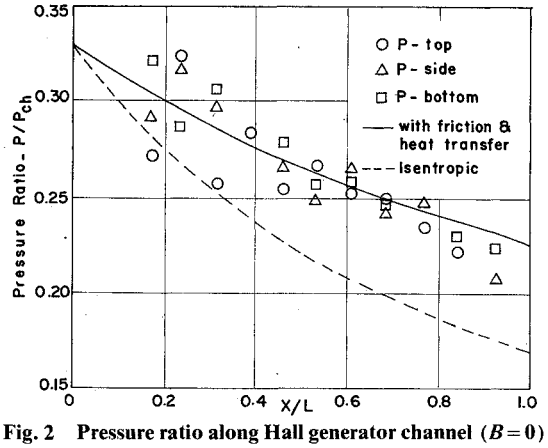

Fig. 2 Pressure ratio along Hall generator channel ($B = 0$).

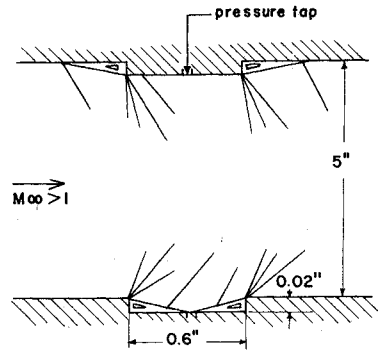

Fig. 3 Schematic wave system of one electrode element.

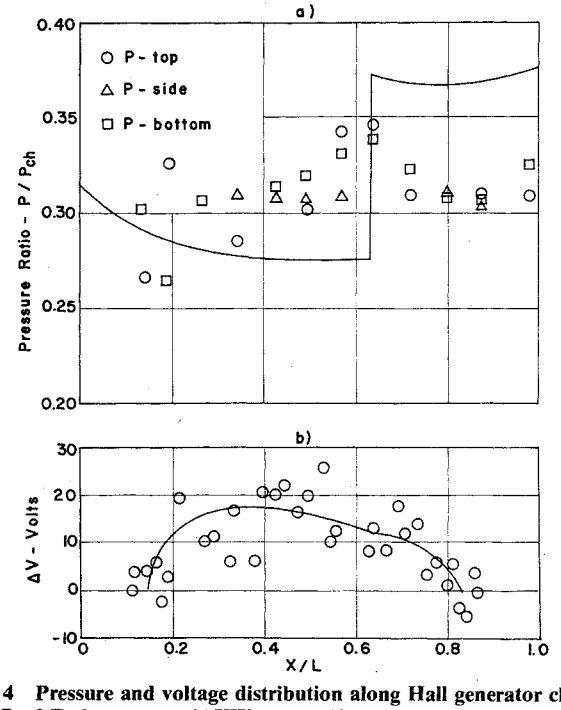

Fig. 4 Pressure and voltage distribution along Hall generator channel ($B = 2$ Tesla, power = 11 KW, load = 10 ohms)

measure a lower value than at the top. The relevant step height for the wave system is the ratio of the step height and boundary-layer thickness. This dimensionless step height decreases along the channel due to boundary-layer growth. This is clearly shown on Fig. 2, as the pressure spread narrows with distance. This figure also gives evidence of extremely thin boundary layer resulting from high cooling rates.

Based on the quasi-one-dimensional equations given previously, the pressure distribution is calculated as shown by the solid line on Fig. 2. The segmentation roughness distributes randomly along the generator channel and its distribution changes during every assembly. Therefore, it is necessary to determine an effective roughness height from pressure distribution. The non-MHD pressure distribution is used to determine this empirical factor which then will remain unchanged when MHD effects are present. The effective roughness height determined here is 0.25 mm. On the same graph, an isentropic (with chemical reaction) pressure distribution is also presented by the dash line. Difference between the experimental value and the isentropic pressure distribution indicates the strong frictional losses despite the high cooling rate existing in the channel.

The non-MHD pressure distribution along the 45° and 60° DCW generators were also measured. The pressure trends are the same as the Hall channel. However, the top and bottom pressure taps are no longer located on the same electrode element; hence no correlation of top and bottom pressures can be found.

B. Hall Channel

The pressure distribution and Hall voltage generated by two electrodes along the Hall generator under load were measured. Figures 4a and 4b show a 10 ohm load condition. We again see the pressure difference between the top (cathode) and bottom (anode) pressure taps. As shown in Fig. 4a, the pressure along the generator channel is very much different from the non-MHD case. The high pressure (relative to non-MHD case) was not expected since only very weak MHD interactions existed. The flow becomes subsonic toward the downstream end of the active generator section. Shock systems were also observed at the same interaction parameter (0.36) and similar area ratio by Louis, Lothrop, and Brogan.[2]

A normal shock was introduced in the calculation as shown by the solid line in Fig. 4a. The computed pressure distribution shows the trend qualitatively. However, the measured Hall voltage agrees quite well with the computed values. The measured pressure shows a gradual rise which indicates that the shock system in the generator is not a single normal shock, but rather a series of oblique shocks (see Fig. 3). These shocks, due to segmentation roughness are very weak when no MHD effects are present. However, when MHD effects are present, the oblique shocks become stronger. The flow finally becomes subsonic through this series of oblique shocks.

C. DCW Generator Channels

For the 60° DCW generator with two terminal connection, studies were made for the following three different conditions: 1) High B field ($B = 2$T) and normal seed flow (1% K by weight); 2) Low B field ($B = 1.5$T) and normal seed flow; and 3) High B field and low seed flow (0.25% K by weight).

At high magnetic field strength (2 Tesla) and normal seed flow rate, the pressure along the channel depends mainly on the load and only to a lesser extent on the power output. Figure 5 shows plots of pressure and Hall voltage for a 4 ohm load. The pressure rise increases with increasing load. It was observed that the pressure peak becomes more pronounced and moves toward upstream direction as load increases. This can be explained partially from current nonuniformities. In Ref. 4, the current distribution on electrode walls in the flow direction was presented. It was found that current concentration at the downstream end of cathode and upstream end of anode increases with load. The high local current den-

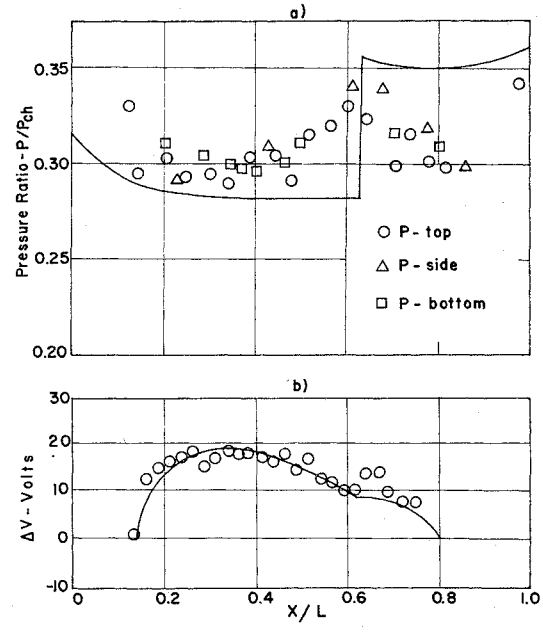

Fig. 5 Pressure and voltage distribution along 60° DCW generator channel ($B = 2$ Tesla, power = 26.4 KW, load = 4 ohms)

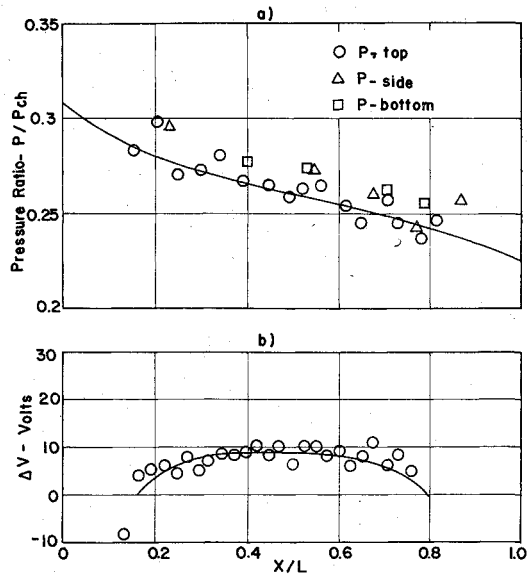

Fig. 6 Pressure and voltage distribution along 60° DCW generator channel ($B = 1.5$ Tesla, power = 9 KW, load = 2.5 ohms).

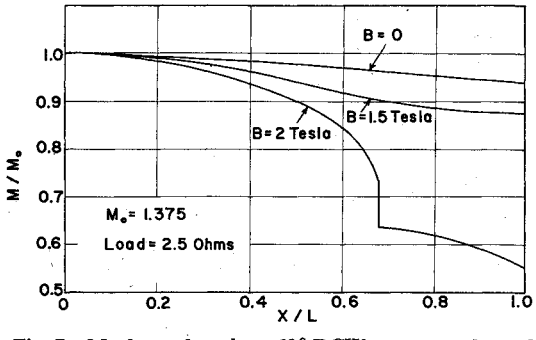

Fig. 7 Mach number along 60° DCW generator channel.

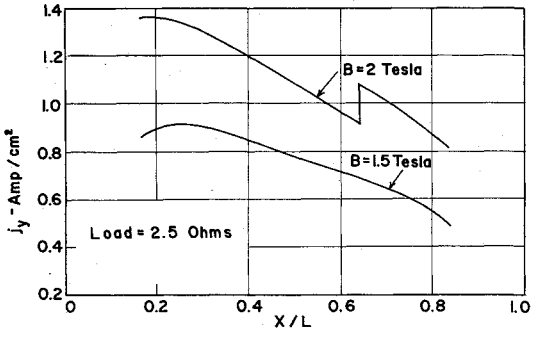

Fig. 8 j_y along 60° DCW generator channel.

sities produce higher local interactions, hence higher pressures. In addition, the transverse current density increases with load. Therefore, higher loads result in larger retarding Lorentz force. This in turn will enhance the MHD interaction.

At either low magnetic field or low seed concentration, favorable pressure gradients always exist throughout the generator channel. Figure 6 shows one of the low B-field cases. In this instance we find the comparison with theory of both the pressure and Hall voltage to be very good. Low seed flow cases also give similar agreement.

Figures 7-9 show the Mach number, current density and temperature, respectively, along the channel for the 60° DCW generator at $B = 2$T and 1.5T with a 2.5 ohm load. Comparison with the non-MHD condition are also shown in Figs. 7 and 9 (normalized with reference to the entrance conditions). The skin friction is causing a slight decrease in the

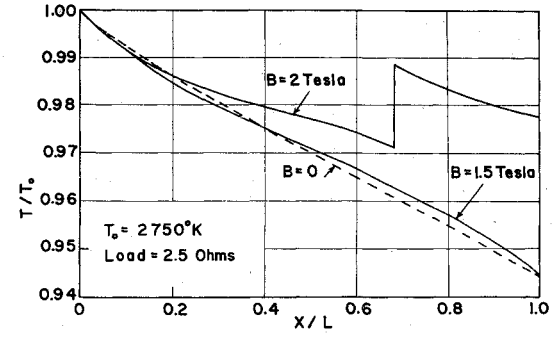

Fig. 9 Temperature along 60° DCW generator channel.

Mach number despite the high cooling rate and increasing area. The presence of MHD effects further decrease the Mach number and at high MHD interactions, a significant reduction in Mach number is noticed and the flow becomes subsonic.

The 45° DCW generator was connected by multiple loads rather than two-terminal. The power output and pressure distribution are very similar to the 60° generator.

The friction factor, which decreases slightly from 0.008444 to 0.008393 remains virtually invariant with B field. This results from the moderate interaction parameter, which is 0.36 and 0.20 for the high (2T) and low (1.5T) B field cases, and very cold boundary layers. The high friction factor was discovered by several investigators.[2,8,9] In a MHD generator, the friction factor can be 3 times higher than those on a smooth wall.[8] Slightly higher friction is expected due to segmentation roughness. However, drastically higher friction is unreasonable with weak MHD interactions. Upon closer examination, it was found that the value of the friction factor used in MHD generators is misleading.[10] Since the MHD generator is a duct, it is common to use average flow parameters, such as velocity, as the reference conditions instead of the freestream conditions normally used in boundary-layer flows. Schlichting[11] has shown that for an incompressible fully developed pipe flow, the mean and maximum velocity ratio depends on the exponent of the velocity profile,

$$(\bar{u}/u_\infty) = 2n^2/[(n+1)(2n+1)]$$

where the velocity profile is approximated by

$$(u/u_\infty) = (y/R)^{1/n}$$

Therefore, for $n = 7$, $\bar{u}/u_\infty = 0.817$. For rough walls, n will decrease, hence $\bar{u}/u_\infty$. This is the reason for the unreasonably large friction factor. Recent studies by Zankl, Raeder, and Bunde[10] proved this point.

The Mach number in the generator channel is moderately low. Therefore, the shock waves are very weak. Furthermore, the generator walls (both sidewalls and electrode walls) were highly cooled. Therefore, the boundary layers are expected to be very thin. Thus, the existance of the shock systems and shock wave boundary-layer interaction played a relatively small role in the effect on power generation. This fact is demonstrated in the voltage distribution along the generator channel when shock waves exist. However, with thick boundary layers and/or stronger shocks, the presence of shocks in the generator channel are detrimental to the generator performance.[2,12]

To maintain high power output of a supersonic generator channel, it must be shock free. The use of an efficient diffuser can greatly improve the generator flow and, hence, its performance. Therefore, the diffuser must be considered as an integral part of the generator.

V. Conclusion

Experimental and theoretical investigations were made of three heat-sink type DCW generators with identical inside

dimensions except the sidewall angles, which are 45°, 60°, and 90° (Hall), respectively. It was found that at low MHD interactions, the pressure gradients remain favorable throughout the entire generator channel. The quasi-one-dimensional analysis gives extremely good agreement on both pressure and Hall voltage distribution along the generator channel. However, at higher interactions, adverse pressure gradients exist in part of the channel. In fact the pressure measurements indicate the existence of subsonic flows toward the downstream end of the channel. The subsonic flow region moves toward upstream as the load increases. The higher pressure rises (relative to the non-MHD case) at higher interactions are not caused by the MHD effect alone, but are also the result of aerodynamic phenomenon resulting from boundary-layer growth and connecting the MHD generator with a downstream diffuser.

Improvement of the generator performance can be made by eliminating the shock system in the generator channel. This can be achieved by a combination of increased mass flow, larger area ratio and improved diffuser design.[2]

References

[1] Louis, J. F., Gal, G., and Black, P. R., "Detailed Theoretical and Experimental Study on a Large MHD Generator," AVCO Research Rept. 174, March 1964.

[2] Louis, J. F., Lothrop, J., and Brogan, T. R., "Fluid Dynamic Studies with Magnetohydrodynamic Generator," *Physics of Fluids*, Vol. 7, No. 3, March 1964, p. 362.

[3] Self, S. A., "Laser Doppler Velocimetry in MHD Boundary Layers," *Proceedings of the 14th Symposium on Engineering Aspects of MHD*, University of Tennessee Space Institute, Tullahoma, Tenn., 1974.

[4] Wu, Y. C. L., et al., "Theoretical and Experimental Studies of Magnetohydrodynamic Power Generation with Char," *Proceedings of the 12th Symposium on Engineering Aspects of MHD*, Argonne National Lab., Argonne, Ill., 1972.

[5] Wu, Y. C. L., Rajagopal, G., and Dicks, J. B., "Investigation of Open-Cycle Magnetohydrodynamic Power Generation," AIAA Paper 74-125, Washington, D.C., Jan. 1974.

[6] Sood, N. S. and Jousson, V. K., "Some Correlations for Resistances to Heat Sublayer at Rough Walls," *Journal of Heat and Mass Transfer*, Vol. 91, No. 4, Ser. C., Nov. 1969, p. 488.

[7] Wu, Y. C. L., et al, "MHD Generator in Two-Terminal Operation," *AIAA Journal*, Vol. 6, Sept. 1968, pp. 1651-1657.

[8] Zankl, G., Raeder, J., and Bunde, R., "The Influence of Various Loss Mechanisms on the Flow Parameters of a Seeded Combustion Plasma," *Proceedings of the 12th Symposium on Engineering Aspects of MHD*, Argonne National Lab., Argonne, Ill., 1972.

[9] Teno, J., Liu, T. R., and Brogan, T. R., "Boundary Layers in MHD Generators," *Proceedings of the 10th Symposium on Engineering Aspects of MHD*, MIT, Cambridge, Mass., 1969.

[10] Zankl, G., Raeder, J., and Bunde, R., "Results of the IPP Test Generator and the Design of a 10 MW_{el} Short-Time Combustion MHD Generator," *Proceedings of the 14th Symposium on Engineering Aspects of MHD*, University of Tennessee Space Institute, Tullahoma, Tenn., 1974.

[11] Schlichting, H., *Boundary Layer Theory*, Pergamon Press, New York, 1955, p. 402.

[12] Dicks, J. B., et al., "MHD Direct Energy Conversion," UTSI 13th Quarterly Rept., Oct. 31, 1974, University of Tennessee Space Institute, Tullahoma, Tenn.